

This discussion paper is/has been under review for the journal Atmospheric Chemistry and Physics (ACP). Please refer to the corresponding final paper in ACP if available.

# Biomass burning related ozone damage on vegetation over the Amazon forest

F. Pacifico<sup>1</sup>, G. A. Folberth<sup>2</sup>, S. Sitch<sup>3</sup>, J. M. Haywood<sup>1,2</sup>, P. Artaxo<sup>4</sup>, and L. V. Rizzo<sup>5</sup>

<sup>1</sup>College of Engineering, Mathematics and Physical Sciences, University of Exeter, Exeter, UK

<sup>2</sup>Met Office Hadley Centre, Exeter, UK

<sup>3</sup>Geography, College of Life and Environmental Sciences, University of Exeter, Exeter, UK

<sup>4</sup>Department of Applied Physics, Institute of Physics, University of Sao Paulo, Sao Paulo, Brazil

<sup>5</sup>Department of Earth and Exact Sciences, Institute of Environmental, Chemical and Pharmaceutics Sciences, Federal University of Sao Paulo, Sao Paulo, Brazil

Received: 5 June 2014 – Accepted: 16 July 2014 – Published: 1 August 2014

Correspondence to: F. Pacifico (f.m.pacifico@exeter.ac.uk)

Published by Copernicus Publications on behalf of the European Geosciences Union.

19955

## Abstract

The HadGEM2 Earth System climate model was used to assess the impact of biomass burning on surface ozone concentrations over the Amazon forest and its impact on vegetation. Simulated surface ozone concentration is evaluated against observations taken at two sites in the Brazilian Amazon forest. The model is able to reproduce the observed diurnal cycle of surface ozone mixing ratio at the two sites, but overestimates the magnitude of the monthly averaged hourly measurements by 5–15 ppb for each available month at one of the sites. We vary biomass burning emissions over South America by  $\pm 20$ , 40, 60, 80 and 100 % to quantify the modelled impact of biomass burning on surface ozone concentrations and ozone damage on vegetation productivity over the Amazon forest. Decreasing South American biomass burning emissions by 100 % (i.e. to zero) reduces surface ozone concentrations and suggests a 15 % increase in monthly mean net primary productivity averaged over the Amazon forest, with local increases up to 60 %: this gives us an estimate of the effect of current biomass burning on plant productivity. When biomass burning emissions are increased by 100 %, our model simulates a maximum impact of 10 % reduction in monthly mean net plant productivity averaged over the Amazon forest, with local peaks of 50–60 % reduction for the months of intense fire activity.

## 1 Introduction

Biomass burning is a global source of aerosol and trace gases, including ozone ( $O_3$ ) precursors, and can lead to local and regional  $O_3$  pollution. Tropospheric  $O_3$  is a greenhouse gas and, above background concentrations, an air pollutant: it is harmful to human health (e.g. Lippmann 1993; Burnett et al., 1997) and it damages plants (e.g. Rich et al., 1964; Fiscus et al., 2005; Felzer et al., 2007; Ainsworth et al., 2012). Tropospheric  $O_3$  is a product of photochemical reactions whose main precursors are nitrogen oxides ( $NO_x$ ), carbon monoxide (CO), methane ( $CH_4$ ) and volatile organic compounds (VOCs)

19956

(Seinfeld and Pandis, 1998). VOCs are particularly important in Amazonia because of the large natural biogenic and biomass burning emissions (Karl et al., 2007).

In the Amazon forest, biomass burning is mostly anthropogenic, and mainly occurs during the dry season (August to October). Biomass burning emissions drastically change the composition of the atmosphere, e.g. diurnal maximum mixing ratios of tropospheric O<sub>3</sub> varies from 12 parts per billion (ppb), during the wet season, to values as high as 100 ppb in the biomass burning affected dry season (Kirkman et al., 2002; Sigler et al., 2002; Artaxo et al., 2002, 2005; Rummel et al., 2007).

Surface O<sub>3</sub> mixing ratios over 40 ppb are known to produce visible leaf injury and damage to plants, reducing crop productivity and posing a threat to food security; nonetheless different climatic conditions (e.g. soil moisture and water stress) also play a role in determining leaf stomatal closure and hence there will be variable impacts of the same O<sub>3</sub> concentrations (Ashmore, 2005). In leaves, cellular damage caused by O<sub>3</sub> not only reduces photosynthetic rates but also requires increased resource allocation to detoxify and repair leaves (Ainsworth et al., 2012). Ozone damage to vegetation reduces plant productivity, decreasing the amount of carbon absorbed by plants, hence has an impact on climate via an indirect radiative forcing (Sitch et al., 2007).

Tropical rain forests play an important role in the global carbon budget, as they cover 12 % of the Earth's land surface and contain around 40 % of the terrestrial biosphere's carbon (Ometto et al., 2005; Taylor and Lloyd, 1992). It has been estimated that they may account for as much as 50 % of the global net primary productivity (Grace et al., 2001). Depending on age, land use and large scale meteorological conditions, tropical forest ecosystems can act as net carbon sources, sinks, or they can be in approximate balance (Lloyd et al., 2007; Gatti et al., 2013), but it is uncertain if global environmental changes are forcing these ecosystems outside their range of natural variation (Sierra et al., 2007). However, biomass burning may further reduce natural sinks in the neighbouring intact forest, via air pollution and O<sub>3</sub> damage on vegetation, and thus current estimates of the effects of biomass burning on the carbon cycle may be underestimated (Le Quéré et al., 2009). Biomass burning is also an important aerosol source: regional

19957

levels of particulate matter are very high in the dry season in Amazonia (Artaxo et al., 2013), and the increase in diffuse radiation due to changes in aerosol loadings can increase net ecosystem exchange (NEE) quite significantly (Oliveira et al., 2007; Cirino et al., 2013). After a certain level of aerosol optical depth, the decrease in radiation fluxes can reduce significantly NEE over Amazonia (Cirino et al., 2013).

Importantly, Sitch et al. (2007) performed their assessment of the potential impact of O<sub>3</sub> on vegetation using an offline simulation where monthly mean O<sub>3</sub> concentrations derived with a global chemistry climate model were used in determining the impacts of O<sub>3</sub> damage. Here we use an online approach to quantify the impact of biomass burning on surface O<sub>3</sub> concentration and O<sub>3</sub> damage on vegetation over the Amazon forest. The HadGEM2 (Hadley Centre Global Environment Model 2; Collins et al., 2011; Martin et al., 2011) Earth System climate model is used to study these interactions. We show results of the evaluation of surface O<sub>3</sub> simulated with HadGEM2 against observations in the Amazon forest and model experiments quantifying the impact of biomass burning on plant productivity.

## 2 Methods

We used HadGEM2 to simulate surface O<sub>3</sub> concentrations and O<sub>3</sub> damage on vegetation for present-day (2001–2009) climate conditions. Our version of HadGEM2 includes the O<sub>3</sub> damage scheme developed by Sitch et al. (2007). We evaluated simulated surface O<sub>3</sub> against observations taken at two sites in the Amazon forest: Porto Velho (Brazil; 8.69° S; 63.87° W), a site heavily impacted by biomass burning emissions, and site ZF2 in the Cuieiras forest reserve in Central Amazonia (Brazil; 2.59° S; 60.21° W). A description of the sites can be found in Artaxo et al. (2013). In a sensitivity study we varied biomass burning emissions over South America by ±20, 40, 60, 80, 100 % to quantify the potential impact of biomass burning on surface O<sub>3</sub> concentrations and O<sub>3</sub> damage over the Amazon forest.

19958

### 3 Model description

HadGEM2 is a fully coupled Earth-system model (Collins et al., 2011). It is built around the HadGEM2 atmosphere-ocean general circulation model and includes a number of earth system components: the ocean biosphere model diat-HadOCC (Diatom-Hadley Centre Ocean Carbon Cycle, a development of the HadOCC model of Palmer and Totterdell, 2001), the Top-down Representation of Interactive Foliage and Flora Including Dynamics (TRIFFID) dynamic global vegetation model (Cox, 2001), the land-surface and carbon cycle model MOSES2 (Met Office Surface Exchange Scheme; Cox et al., 1998, 1999; Essery et al., 2003), the interactive Biogenic Volatile Organic Compounds (iBVOC) emission model (Pacifico et al., 2012), the UK Chemistry and Aerosol (UKCA) model (O'Connor et al., 2014) and an interactive scheme of O<sub>3</sub> damage on vegetation (Sitch et al., 2007; Clark et al., 2011).

The configuration used here is a version of HadGEM2-UKCA with extended tropospheric chemistry (N96L38), the resolution is 1.25° latitude × 1.875° longitude (~200 km × 140 km) with 38 vertical levels extending up to 39 km altitude. The land-based anthropogenic, biomass burning, and shipping emissions are taken from Lamarque et al. (2010), and represent a decadal (1997–2006) mean centered on the year 2000. The use of an emission pattern from 1997–2006 can lead to an overestimation of O<sub>3</sub> concentrations by the model, since the emissions vary on a year to year basis and are expected to be lower in recent years due to the reduction in Amazonian deforestation. HadGEM2 runs at a 30 min time step with the exception of global radiation, which is updated every 3 h and provides radiative fluxes between those time steps via interpolation. This configuration is described and evaluated in O'Connor et al. (2014) with the exception of the Extended Tropospheric Chemistry (ExtTC) that has been applied in this work. The ExtTC mechanism has been designed to represent the key species and reactions in the troposphere in as much detail as is necessary to simulate atmospheric composition-climate couplings and feedbacks while retaining the capability to conduct decade-long climate simulations. UKCA-ExtTC simulates the spatial distribu-

19959

tion and evolution in time of 89 chemical species, 63 of which are model tracers. The model includes emissions from anthropogenic, biogenic, soil, and wildfire sources for 17 species: nitrogen oxides (NO<sub>x</sub> = NO + NO<sub>2</sub>), CH<sub>4</sub>, carbon monoxide (CO), hydrogen (H<sub>2</sub>), methanol, formaldehyde, acetaldehyde and higher aldehydes, acetone, methyl ethyl ketone, ethane (C<sub>2</sub>H<sub>6</sub>), propane (C<sub>3</sub>H<sub>8</sub>), butanes and higher alkanes, ethene (C<sub>2</sub>H<sub>4</sub>), propene (C<sub>3</sub>H<sub>6</sub>), isoprene, (mono)terpenes, and a lumped species representing aromatics (toluene + xylene) from anthropogenic sources.

Emissions of biogenic species (isoprene, terpenes, methanol, acetone) are computed by iBVOC and provided to UKCA at every time step. The isoprene emission scheme is that of Pacifico et al. (2011). Terpenes, methanol, and acetone emissions are simulated with the model described in Guenther et al. (1995). Anthropogenic and wildfire emissions are prescribed from monthly mean emission data sets prepared for CMIP5 using the historic scenario (Lamarque et al., 2010), while wetland methane emissions are prescribed from data from Gedney et al. (2004). Soil-biogenic NO<sub>x</sub> emissions are prescribed using the monthly distributions provided by the Global Emissions Inventory Activity (<http://www.geiacenter.org/inventories/present.html>), which are based on the global empirical model of soil-biogenic NO<sub>x</sub> emissions of Yienger and Levy (1995). NO<sub>x</sub> emissions from global lightning activity are parameterized based on the convective cloud top height following Price and Rind (1992, 1994) and are thus sensitive to the model climate. UKCA also includes a dry deposition scheme based on the resistance in-series approach as outlined in Wesely (1989). Physical removal of soluble species is parameterized as a first-order loss process based on convective and stratiform rainfall rates (Collins et al., 2011).

The TRIFFID vegetation module of HadGEM2 simulates the dynamics of five plant functional types (PFTs): broadleaf trees, needleleaf trees, shrubs, and C<sub>3</sub> and C<sub>4</sub> grass (i.e., grasses using the C<sub>3</sub> and C<sub>4</sub> photosynthetic pathway, respectively). Changes in the extent of croplands over time are not simulated but are prescribed from land use maps prepared for the Coupled Model Intercomparison Project 5 (CMIP5, Taylor et al., 2012). Here we use the historic (1850–2000; Hurtt et al., 2009) data sets, as described

19960





55–60 ppb in this region (Fig. 4), while the average over the region of analysis is peaked at about 30 ppb in August and September, less in October (Fig. 5a, black line).

Monthly total Net Primary Productivity (NPP) in our control simulation reaches its minimum during the months of August and September (Fig. 5b, black line), at about 5 300 Tg C month<sup>-1</sup>, corresponding to the end of the dry season.

Decreasing biomass burning emissions over South America by –20 %, –40 %, –60 %, –80 %, –100 % decreases surface O<sub>3</sub> mixing ratios and increases net productivity. Vice versa, increasing biomass burning emissions over South America by +20 %, +40 %, +60 %, +80 %, +100 % increases surface O<sub>3</sub> mixing ratios over the 10 region of analysis and subsequently reduces net productivity because of O<sub>3</sub> damage on vegetation (Fig. 5c).

These sensitivity tests suggest that decreasing biomass burning emission by 100 % over South America brings monthly mean surface O<sub>3</sub> mixing ratios averaged over the region of analysis to about the observed 15 ppb for each month (Fig. 5a, dark blue 15 line), even during the dry season, with no values over 35 ppb for any grid-cell (Fig. 6). Increasing biomass burning emissions by 100 % suggests that monthly mean mixing ratios of surface O<sub>3</sub> averaged over the region of analysis reach 40 ppb in August (Fig. 5a), with peaks of about 65–70 ppb in some grid-cells (Fig. 6a). For both increases and decreases of between 20 and 80 % in South American biomass burning the model 20 simulates almost linear changes in surface O<sub>3</sub> mixing ratios (Fig. 6, the figure shows increases and reductions by 40, 60 and 100 %).

Suppressing biomass burning emissions (i.e. decreasing biomass burning emission by 100 %) over South America increases total NPP over the region of analysis by about 15 %, to about 350–370 Tg C month<sup>-1</sup>, with peak increases of 60 % for a few grid-cells, 25 in August and September (Fig. 6b): this quantifies the impact of present-day biomass burning on vegetation productivity. When increasing biomass burning emissions over South America by 100 %, monthly total NPP over the region of analysis is reduced by about 10 %, i.e. to about 250 Tg C month<sup>-1</sup>, in August and September (Fig. 5b), with peak values of 50–60 % reductions for a few grid-cells (Fig. 6c). For reductions by

19965

20 to 80 % in South American biomass burning the model varies NPP almost linearly (Fig. 5c). However, the increase in South American biomass burning by 20 to 80 % determine a very similar decrease in NPP, e.g. between 7 and 10 % decrease in August (Fig. 5c). Both increasing and reducing South American biomass burning from 20 to 5 80 % increases the number of grid-cells where a significant variation of NPP takes place (Fig. 6b). The percentages given above are significant against variability in the control simulation, i.e. we only take into account of the variations above one standard deviation in the control simulation. We also exclude from our analysis the gridcells with low productivity, i.e. where NPP in the control simulation is below 50 g C m<sup>-2</sup> month<sup>-1</sup> 10 (i.e. forest, high productivity regions).

## 7 Discussion and conclusions

The HadGEM2 model overestimates the magnitude of the O<sub>3</sub> diurnal cycle at the two sites used in the evaluation. Overestimation of simulated O<sub>3</sub> in the Amazonian boundary layer has been observed in other modelling studies, especially in clean air conditions (Bela et al., 2014). Nonetheless, our model reproduces the main features of the 15 diurnal and seasonal cycle. In particular, the model is able to reproduce the increase in surface O<sub>3</sub> during the biomass burning season.

The model overestimates surface O<sub>3</sub> mixing ratios by 5–15 ppb for several months at the ZF2 site in the Cuieiras forest reserve and for all available months at the Porto Velho site. The reasons for these systematic biases in surface O<sub>3</sub> mixing ratio are likely manifold. In a complex, highly coupled system such as the HadGEM2 Earth System Model (ESM) it is not always easy to disentangle all processes and attribute model 20 biases to specific components, however, it is not altogether impossible.

We attribute the systematic biases in the surface O<sub>3</sub> mixing ratio to the following, 25 most likely reasons:

1. Model resolution in both the horizontal and the vertical dimension

19966

2. Uncertainties in emissions, both magnitude, seasonality and location

3. Uncertainties in the O<sub>3</sub> dry deposition at the surface

Other factors such as photolysis rates, lightning NO<sub>x</sub> production over the area and transport of O<sub>3</sub> and precursors will certainly contribute. We will briefly discuss the three most important (in our opinion) factors that contribute to the systematic biases.

The relatively coarse resolution of a global ESM simulates mixing ratios of trace species (both trace gases and aerosols) that represent averages over large areas. This issue has been discussed previously in the literature, mostly in relation to air quality modelling (see, e.g., Valari and Menut, 2008; Tie et al., 2010; Appel et al., 2011; Thompson and Selin, 2012). In our case one grid box equals approximately 30 000 km<sup>2</sup> (i.e., 200 km × 150 km in longitude and latitude). The implicit averaging pertains both to emission and concentration fields; the predominant consequence is a dilution in each grid-cell. Depending on the chemical regime, this can lead to reduced or enhanced net O<sub>3</sub> production. Additionally, HadGEM2-ES has a relatively coarse vertical resolutions. HadGEM2-ES has a lowest model layer depth of 48 m (global average) and the vertical profile of O<sub>3</sub> will undoubtedly show a gradient as the loss mechanism for O<sub>3</sub> is dominated by the surface (e.g. Colbeck and Harrison, 1967).

The remote environment of the Amazon forest is dominated by relatively high concentrations of VOC, particularly of biogenic origin, and low concentrations of nitrogen oxides, NO<sub>x</sub>. It is a NO<sub>x</sub>-limited environment. In such an environment O<sub>3</sub> is destroyed by reactions with bVOC (mainly isoprene and (mono-)terpenes). This destruction is more pronounced the higher the bVOC concentration becomes. Consequently, conditions in the global model are likely to differ from that of a measurement at a specific point such as those we compare to in Figs. 1 and 2. It is a known problem in model evaluation.

Another issue related to model resolution, when comparing global models to point-like observations, is the uncertainty in global emission inventories, both with respect to magnitude and location. In particular the latter will result in discrepancies between

19967

modelled concentrations of O<sub>3</sub> and its precursors and point-like observations. But the uncertainties in emission magnitude are also substantial and can reach a factor of two or more in case of biogenic VOC (e.g., Guenther et al., 2006; Arneth et al., 2008, 2011; Pacifico et al., 2011, 2012).

Thirdly, and again related to model resolution, is the representation of O<sub>3</sub> dry deposition at the surface. Its magnitude and diurnal cycle will depend on boundary layer turbulence, surface roughness, land surface type, vegetation type, soil moisture, photosynthetic activity, and more. In a recent sensitivity study by Folberth et al. (2014) O<sub>3</sub> surface concentrations showed the largest sensitivity to perturbations in O<sub>3</sub> surface dry deposition fluxes. Underestimating O<sub>3</sub> surface dry deposition, in particular during the night preventing a complete flush of the planetary boundary layer with respect to O<sub>3</sub>, will lead to systematic biases.

Interestingly, however, the latter process may also represent a redeeming feature of the model. According to our model of O<sub>3</sub> plant damage, it is the total O<sub>3</sub> flux into the plant that determines the amount of damage caused to the photosynthetic activity and, hence, carbon assimilation. However, the total O<sub>3</sub> flux (or dose) is a function of both O<sub>3</sub> surface concentrations and dry deposition. Underestimating the O<sub>3</sub> dry deposition flux not only leads to a positive bias in the O<sub>3</sub> concentration, and consequently an underestimation of the damage caused by O<sub>3</sub>, but also to a negative bias in the O<sub>3</sub> plant uptake, and consequently an underestimation of the plant damage. Still, a detailed assessment and quantification of this interdependence of O<sub>3</sub> concentration and dry deposition fluxes is beyond the scope of this study and must be referred to future research.

August, September and October are the months when biomass burning and surface O<sub>3</sub> concentrations are higher over the Amazon forest, but also the months when plant productivity is at its lowest which will tend to suppress the impact of O<sub>3</sub> damage on plant productivity. This is because stomatal conductance is reduced due to water limitations (also accounted for in the model) during the dry season, thus reducing the flux of both carbon dioxide and O<sub>3</sub> into the leaves, and consequently reducing O<sub>3</sub> plant damage.

19968

Ashmore (2005), noted how  $O_3$  exposure is poorly correlated with flux into leaves and also the potential for damagingly high  $O_3$  fluxes in leaves at concentrations significantly below 40 ppb at maximum stomatal conductance. Consequently, global vegetation models as used in this study have adopted flux-based parameterizations to represent  $O_3$  impacts on vegetation, moving away from application of the earlier exposure based metrics, e.g. accumulated  $O_3$  exposure above a threshold of 40 ppb, AOT40. Consequently we simulate  $O_3$  damage on vegetation even for lower surface  $O_3$  mixing ratios (e.g. less than 40 ppb) due to higher stomatal conductances associated with tropical forests. Moreover, tropical vegetation could be more sensitive to  $O_3$  damage as it evolved in low background  $O_3$ .

The parameterization of  $O_3$  damage used in this study is calibrated for high-latitude vegetation. Unfortunately data for calibrating this  $O_3$  damage scheme for tropical vegetation are currently not available and observations of  $O_3$  damage in the Amazon forest are very limited. Observations of  $O_3$  damage on tropical forests are urgently needed, including observations at moderate (e.g. 20–30 ppb) and high surface  $O_3$  mixing ratios.

The simulated impact of present-day biomass burning on vegetation productivity is about  $230 \text{ Tg C yr}^{-1}$  (i.e. the difference between the dark blue line and the black line in Fig. 5b). Taking into account that the uncertainty in these estimates is substantial, this  $O_3$  damage impact over the Amazon forest is of the same order of magnitude of the release of  $CO_2$  due to land fire in South America, as quantified in van der Werf et al. (2010;  $293 \text{ Tg C yr}^{-1}$  from Table 7 of that paper); in effect to potentially double the impact of biomass burning on the carbon cycle. This highlights the urgent need for more tropical data on plant  $O_3$  damage to better constrain estimates.

Despite overestimating surface  $O_3$  mixing ratios our model simulates only a moderate reduction in NPP associated with elevated  $O_3$  due to biomass burning emissions. Given that our model systematically overestimates  $O_3$  mixing ratio, assuming accurate dry deposition, and that we use our model in the high sensitivity mode, our simulations where we increase biomass burning emissions by 100 % suggest a maximum 10 % average reduction in monthly plant productivity, and peak reductions of 50–60 % re-

19969

ductions in few grid-cells. This is because, despite the increase in biomass burning, monthly average surface  $O_3$  mixing ratios do not exceed a moderate 40 ppb. Moreover, our model does not include deforestation due to fire, which would reduce vegetation cover when increasing biomass burning emissions in our sensitivity experiments, reducing NPP further. However, local and daily/hourly impact of  $O_3$  damage on plant productivity can be higher.

Estimates of the magnitude of the reduction in plant productivity due to  $O_3$  damage can be improved with additional field studies and improving the representation of tropospheric  $O_3$  in ESMs (sources, chemistry and sinks). Nevertheless, considering these processes in a coupled system can provide an improvement in robustness of conclusions, as e.g. it can treat processes with a specific diurnal cycle, like photosynthesis and surface  $O_3$ , interactively on a short time scale (e.g. half an hour in our model).

*Acknowledgements.* This work was funded by the Natural Environment Research Council (NERC) South American Biomass Burning Analysis (SAMBBA) project grant code NE/J010057/1. The UK Met Office contribution to this project was funded by the DECC under the Hadley Centre Climate Programme contract (GA01101). The Brazilian contribution was funded by Fundacao de Amparo a Pesquisa do Estado de Sao Paulo (FAPESP, projects 08/58100-2 and 12/14437-9). We thank INPA (Instituto Nacional de Pesquisas da Amazonia) for the coordination work of the LBA Experiment. We thank USP technicians for the support on data sampling: Alcides Ribeiro, Ana Lucia Loureiro, Fernando Morais and Fabio Jorge.

## References

- Ainsworth, E. A., Yendrek, C. R., Sitch, S., Collins, W. J., and Emberson, L. D.: The effects of tropospheric ozone on net primary productivity and implications for climate change, *Annu. Rev. Plant Biol.*, 63, 637–61, 2012.
- Appel, K. W., Foley, K. M., Bash, J. O., Pinder, R. W., Dennis, R. L., Allen, D. J., and Pickering, K.: A multi-resolution assessment of the Community Multiscale Air Quality (CMAQ) model v4.7 wet deposition estimates for 2002–2006, *Geosci. Model Dev.*, 4, 357–371, doi:10.5194/gmd-4-357-2011, 2011.

19970

- Arneth, A., Monson, R. K., Schurgers, G., Niinemets, Ü., and Palmer, P. I.: Why are estimates of global terrestrial isoprene emissions so similar (and why is this not so for monoterpenes)?, *Atmos. Chem. Phys.*, 8, 4605–4620, doi:10.5194/acp-8-4605-2008, 2008.
- Arneth, A., Schurgers, G., Lathiere, J., Duhal, T., Beerling, D. J., Hewitt, C. N., Martin, M., and Guenther, A.: Global terrestrial isoprene emission models: sensitivity to variability in climate and vegetation, *Atmos. Chem. Phys.*, 11, 8037–8052, doi:10.5194/acp-11-8037-2011, 2011.
- Artaxo, P., Martins, J. V., Yamasoe, M. A., Procópio, A. S., Pauliquevis, T. M., Andreae, M. O., Guyon, P., Gatti, L. V., and Leal, A. M. C.: Physical and chemical properties of aerosols in the wet and dry season in Rondônia, Amazonia, *J. Geophys. Res.*, 107, 8081–8095, 2002.
- Artaxo, P., Gatti, L. V., Leal, A. M. C., Longo, K. M., de Freitas, S. R., Lara, L. L., Pauliquevis, T. M., Procópio, A. S., and Rizzo, L. V.: Atmospheric chemistry in Amazonia: the forest and the biomass burning emissions controlling the composition of the Amazonian atmosphere, *Acta Amazonica*, 35, 185–196, 2005.
- Artaxo, P., Rizzo, L. V., Brito, J. F., Barbosa, H. M. J., Arana, A., Sena, E. T., Cirino, G. G., Bastos, W., Martin, S. T., and Andreae, M. O.: Atmospheric aerosols in Amazonia and land use change: from natural biogenic to biomass burning conditions, *Faraday Discuss.*, 165, 203–235, 2013.
- Ashmore, M. R.: Assessing the future global impacts of ozone on vegetation, *Plant Cell Environ.*, 28, 949–964, 2005.
- Bela, M. M., Longo, K. M., Freitas, S. R., Moreira, D. S., Beck, V., Wofsy, S. C., Gerbig, C., Wiedemann, K., Andreae, M. O., and Artaxo, P.: Ozone production and transport over the Amazon Basin during the dry-to-wet and wet-to-dry transition seasons, *Atmos. Chem. Phys. Discuss.*, 14, 14005–14070, doi:10.5194/acpd-14-14005-2014, 2014.
- Brito, J., Rizzo, L. V., Morgan, W. T., Coe, H., Johnson, B., Haywood, J., Longo, K., Freitas, S., Andreae, M. O., and Artaxo, P.: Ground based aerosol characterization during the South American Biomass Burning Analysis (SAMBBA) field experiment, *Atmos. Chem. Phys. Discuss.*, 14, 12279–12322, doi:10.5194/acpd-14-12279-2014, 2014.
- Burnett, R. T., Brook, J. R., Yung, W. T., Dales, R. E., Krewski, D.: Association between ozone and hospitalization for respiratory diseases in 16 Canadian cities, *Environ. Res.*, 72, 1, 24–31, 1997.
- Cirino, G. G., Souza, R. A. F., Adams, D. K., and Artaxo, P.: The effect of atmospheric aerosol particles and clouds on net ecosystem exchange in the Amazon, *Atmos. Chem. Phys.*, 14, 6523–6543, doi:10.5194/acp-14-6523-2014, 2014.

19971

- Clark, D. B., Mercado, L. M., Sitch, S., Jones, C. D., Gedney, N., Best, M. J., Pryor, M., Rooney, G. G., Essery, R. L. H., Blyth, E., Boucher, O., Harding, R. J., Huntingford, C., and Cox, P. M.: The Joint UK Land Environment Simulator (JULES), model description – Part 2: Carbon fluxes and vegetation dynamics, *Geosci. Model Dev.*, 4, 701–722, doi:10.5194/gmd-4-701-2011, 2011.
- Colbeck, I. and Harrison, R. M.: Dry deposition of ozone: some measurements of deposition velocity and of vertical profiles to 100 metres, *Atmos. Environ.*, 19, 11, 1807–1818, 1967.
- Collins, W. J., Bellouin, N., Doutriaux-Boucher, M., Gedney, N., Halloran, P., Hinton, T., Hughes, J., Jones, C. D., Joshi, M., Liddicoat, S., Martin, G., O'Connor, F., Rae, J., Senior, C., Sitch, S., Totterdell, I., Wiltshire, A., and Woodward, S.: Development and evaluation of an Earth-System model – HadGEM2, *Geosci. Model Dev.*, 4, 1051–1075, doi:10.5194/gmd-4-1051-2011, 2011.
- Cox, P. M.: Description of the “TRIFFID” Dynamic Global Vegetation Model, Tech. Note 24, Met Off. Hadley Cent., Exeter, UK, 17 pp., 2001.
- Cox, P. M., Huntingford, C., and Harding, R. J.: A canopy conductance and photosynthesis model for use in a GCM land surface scheme, *J. Hydrol.*, 212–213, 79–94, 1998.
- Cox, P. M., Betts, R. A., Bunton, C. B., Essery, R. L. H., Rowntree, P. R., and Smith, J.: The impact of new land surface physics on the GCM simulation of climate and climate sensitivity, *Clim. Dynam.*, 15, 183–203, 1999.
- Essery, R. L. H., Best, M. J., Betts, R. A., Cox, P. M., and Taylor, C. M.: Explicit representation of subgrid heterogeneity in a GCM land surface scheme, *J. Hydrometeorol.*, 4, 530–543, 2003.
- Felzer, B., Reilly, J., Melillo, J., Kicklighter, D., Sarofim, M., Wang, C., Prinn, R., and Zhuang, Q.: Future effects of ozone on carbon sequestration and climate change policy using a global biogeochemical model, *Climatic Change*, 73, 345–373, 2005.
- Felzer, B. S., Cronin, T., Reilly, J. M., Melillo, J. M., and Wang, X.: Impacts of ozone on trees and crops, *C. R. Geosci.*, 339, 784–798, 2007.
- Fiscus, E. L., Booker, F. L., Burkey, K. O.: Crop responses to ozone: uptake, modes of action, carbon assimilation and partitioning, *Plant Cell Environ.*, 28, 997–1011, 2005.
- Folberth, G. A., Abraham, N. L., Dalvi, M., Johnson, C. E., Morgenstern, O., O'Connor, F. M., Pacifico, F., Young, P. A., Collins, W. J., and Pyle, J. A.: Evaluation of the new UKCA climate-composition model – Part 4: Extension to tropospheric chemistry and biogeochemical coupling between atmosphere and biosphere, in preparation, *Geosci. Model Dev. Discuss.*, 2014.

19972

- Gatti, L. V., Gloor, M., Miller, J. B., Doughty, C. E., Malhi, Y., Domingues, L. G., Basso, L. S., Martinewski, A., Correia, C. S. C., Borges, V. F., Freitas, S., Braz, R., Anderson, L. O., Rocha, H., Grace, J., Phillips, O. L., and Lloyd, J.: Drought sensitivity of Amazonian carbon balance revealed by atmospheric measurements, *Nature*, 506, 76–80, 2014.
- 5 Gedney, N., Cox, P. M., and Huntingford, C.: Climate feedback from wetland methane emissions, *Geophys. Res. Lett.*, 31, L20503, doi:10.1029/2004GL020919, 2004.
- Grace, J., Malhi, Y., Higuchi, N., and Meir, P.: Productivity and carbon fluxes of tropical rain forest, in: *Global Terrestrial Productivity*, edited by: Roy, J., Saugier, B. and Mooney, H. A., Academic Press, San Diego, 401–426, 2001.
- 10 Guenther, A., Hewitt, C. N., Erickson, D., Fall, R., Geron, C., Graedel, T., Harley, P., Klinger, L., Lerdau, M., McKay, W. A., Pierce, T., Scholes, B., Steinbrecher, R., Tallamraju, R., Taylor, J., and Zimmerman, P.: A global model of natural volatile organic compound emissions, *J. Geophys. Res.*, 100, 8873–8892, 1995.
- Guenther, A., Karl, T., Harley, P., Wiedinmyer, C., Palmer, P. I., and Geron, C.: Estimates of global terrestrial isoprene emissions using MEGAN (Model of Emissions of Gases and Aerosols from Nature), *Atmos. Chem. Phys.*, 6, 3181–3210, doi:10.5194/acp-6-3181-2006, 2006.
- 15 Hurtt, G. C., Chini, L. P., Frolking, S., Betts, R. A., Feddema, J., Fischer, G., Fisk, J. P., Hibbard, K., Houghton, R. A., Janetos, A., Jones, C. D., Kindermann, G., Kinoshita, T., Goldewijk, K. K., Riahi, K., Shevliakova, E., Smith, S., Stehfest, E., Thomson, A., Thornton, P., van Vuuren, D. P., and Wang, Y. P.: Harmonization of global land-use scenarios for the period 1500–2100 for IPCC-AR5, *iLEAPS Newsl.*, 7, 6–8, 2009.
- Jones, C. D., Hughes, J. K., Bellouin, N., Hardiman, S. C., Jones, G. S., Knight, J., Lid-dicoat, S., O'Connor, F. M., Andres, R. J., Bell, C., Boo, K.-O., Bozzo, A., Butchart, N., Cadule, P., Corbin, K. D., Doutriaux-Boucher, M., Friedlingstein, P., Gornall, J., Gray, L., Halloran, P. R., Hurtt, G., Ingram, W. J., Lamarque, J.-F., Law, R. M., Meinshausen, M., Osprey, S., Palin, E. J., Parsons Chini, L., Raddatz, T., Sanderson, M. G., Sellar, A. A., Schurer, A., Valdes, P., Wood, N., Woodward, S., Yoshioka, M., and Zerroukat, M.: The HadGEM2-ES implementation of CMIP5 centennial simulations, *Geosci. Model Dev.*, 4, 543–570, doi:10.5194/gmd-4-543-2011, 2011.
- 20 Karl, T., Guenther, A., Yokelson, R., J., Greenberg, J., Potosnak, M., Blake, D., R. and Artaxo, P.: The tropical forest and fire emissions experiment: Emission, chemistry, and transport of

19973

- biogenic volatile organic compounds in the lower atmosphere over Amazonia, *J. Geophys. Res.*, 112, D18302, doi:10.1029/2007JD008539, 2007.
- Kirkman, G. A., Gut, A., Ammann, C., Gatti, L. V., Cordova, A. M., Moura, M. A. L., and Meixner, F. X.: Surface exchange of nitric oxide, nitrogen dioxide, and ozone at a cattle pas-ture in Rondônia, Brazil, *J. Geophys. Res.*, 107, 8083, doi:10.1029/2001JD000523, 2002.
- 5 Kvalevag M. M. and Myhre, G.: The effect of carbon-nitrogen coupling on the reduced land carbon sink caused by tropospheric ozone, *Geophys. Res. Lett.*, 40, 1–5, 2013.
- Lamarque, J.-F., Bond, T. C., Eyring, V., Granier, C., Heil, A., Klimont, Z., Lee, D., Liousse, C., Mieville, A., Owen, B., Schultz, M. G., Shindell, D., Smith, S. J., Stehfest, E., Van Aar-den, J., Cooper, O. R., Kainuma, M., Mahowald, N., McConnell, J. R., Naik, V., Riahi, K., and van Vuuren, D. P.: Historical (1850–2000) gridded anthropogenic and biomass burn-ing emissions of reactive gases and aerosols: methodology and application, *Atmos. Chem. Phys.*, 10, 7017–7039, doi:10.5194/acp-10-7017-2010, 2010.
- 10 Le Quéré, C. M. R., Raupach, J. G., Canadell, G., Marland, Bopp, L., Ciais, P., Conway, T. J., Doney, S. C., Feely, R. A., Foster, P., Friedlingstein, P., Gurney, K., Houghton, R. A., House, J. I., Huntingford, C., Levy, P. E., Lomas, M. R., Majkut, J., Metzl, N., Ometto, J. P., Peters, G. P., Prentice, I. C., Randerson, J. T., Running, S. W., Sarmiento, J. L., Schuster, U., Sitch, S., Takahashi, T., Viovy, N., van der Werf, G. R., and Woodward, F. I.: Trends in the sources and sinks of carbon dioxide, *Nat. Geosci.*, 2, 831–836, 2009.
- 15 Lippmann, M.: Health effects of tropospheric ozone: review of recent research findings and their implications to ambient air quality standards, *J. Exp. An. Environ. Epid.*, 3, 103–129, 1993.
- Lloyd, J., Kolle, O., Fritsch, H., de Freitas, S. R., Silva Dias, M. A. F., Artaxo, P., Nobre, A. D., de Araújo, A. C., Kruijt, B., Sogacheva, L., Fisch, G., Thielmann, A., Kuhn, U., and And-reae, M. O.: An airborne regional carbon balance for Central Amazonia, *Biogeosciences*, 4, 759–768, doi:10.5194/bg-4-759-2007, 2007.
- 20 Martin, S. T., Andreae, M. O., Althausen, D., Artaxo, P., Baars, H., Borrmann, S., Chen, Q., Farmer, D. K., Guenther, A., Gunthe, S. S., Jimenez, J. L., Karl, T., Longo, K., Manzi, A., Müller, T., Pauliquevis, T., Petters, M. D., Prenni, A. J., Pöschl, U., Rizzo, L. V., Schneider, J., Smith, J. N., Swietlicki, E., Tota, J., Wang, J., Wiedensohler, A., and Zorn, S. R.: An overview of the Amazonian Aerosol Characterization Experiment 2008 (AMAZE-08), *Atmos. Chem. Phys.*, 10, 11415–11438, doi:10.5194/acp-10-11415-2010, 2010.
- 30 Martin, G. M., Bellouin, N., Collins, W. J., Culverwell, I. D., Halloran, P. R., Hardiman, S. C., Hinton, T. J., Jones, C. D., McDonald, R. E., McLaren, A. J., O'Connor, F. M., Roberts, M.

19974

- J., Rodriguez, J. M., Woodward, S., Best, M. J., Brooks, M. E., Brown, A. R., Butchart, N., Dearden, C., Derbyshire, S. H., Dharssi, I., Doutriaux-Boucher, M., Edwards, J. M., Falloon, P. D., Gedney, N., Gray, L. J., Hewitt, H. T., Hobson, M., Huddleston, M. R., Hughes, J., Ineson, S., Ingram, W. J., James, P. M., Johns, T. C., Johnson, C. E., Jones, A., Jones, C. P., Joshi, M. M., Keen, A. B., Liddicoat, S., Lock, A. P., Maidens, A. V., Manners, J. C., Milton, S. F., Rae, J. G. L., Ridley, J. K., Sellar, A., Senior, C. A., Totterdell, I. J., Verhoef, A., Vidale, P. L. and Wiltshire, A.: The HadGEM2 family of Met Office Unified Model climate configurations, *Geosci. Model Dev.*, 4, 723–757, doi:10.5194/gmd-11-723-2011, 2011.
- O'Connor, F. M., Johnson, C. E., Morgenstern, O., Abraham, N. L., Braesicke, P., Dalvi, M., Folberth, G. A., Sanderson, M. G., Telford, P. J., Voulgarakis, A., Young, P. J., Zeng, G., Collins, W. J., and Pyle, J. A.: Evaluation of the new UKCA climate-composition model – Part 2: The Troposphere, *Geosci. Model Dev.*, 7, 41–91, doi:10.5194/gmd-7-41-2014, 2014.
- Oliveira, P. H. F., Artaxo, P., Pires Jr, C., de Lucca, S., Procópio, A., Holben, B., Schafer, J., Cardoso, L. F., Wofsy, S. C., and Rocha, H. R.: The effects of biomass burning aerosols and clouds on the CO<sub>2</sub> flux in Amazonia, *Tellus B*, 59, 338–349, 2007.
- Ometto, J. P., Nobre, A. D., Rocha, H., Artaxo, P., and Martinelli, L.: Amazônia and the modern carbon cycle: lessons learned, *Oecologia*, 143, 483–500, 2005.
- Pacifico, F., Harrison, S. P., Jones, C. D., Arneth, A., Sitch, S., Weedon, G. P., Barkley, M. P., Palmer, P. I., Serça, D., Potosnak, M., Fu, T.-M., Goldstein, A., Bai, J., and Schurgers, G.: Evaluation of a photosynthesis-based biogenic isoprene emission scheme in JULES and simulation of isoprene emissions under present-day climate conditions, *Atmos. Chem. Phys.*, 11, 4371–4389, doi:10.5194/acp-11-4371-2011, 2011.
- Pacifico, F., Folberth, G. A., Jones, C. D., Harrison, S. P., and Collins, W. J.: Sensitivity of biogenic isoprene emissions to past, present, and future environmental conditions and implications for atmospheric chemistry, *J. Geophys. Res.*, 117, D22302, doi:10.1029/2012JD018276, 2012.
- Palmer, J. R. and Totterdell, I. J.: Production and export in a global ocean ecosystem model, *Deep-Sea Res. Pt I*, 48, 1169–1198, 2001.
- Price, C. and Rind, D.: A simple lightning parameterization for calculating global lightning distributions, *J. Geophys. Res.*, 97, 9919–9933, 1992.
- Price, C. and Rind, D.: Modeling global lightning distributions in a general circulation model, *Mon. Weather Rev.*, 122, 1930–1939, 1994.

19975

- Riahi, K., Gruebler, A., and Nakicenovic, N.: Scenarios of long-term socio-economic and environmental development under climate stabilization, *Technol. Forecast. Soc.*, 74, 887–935, 2007.
- Rich, S.: Ozone damage to plants, *Annu. Rev. Phytopathol.*, 2, 253–266, 1964.
- Rizzo, L. V., Artaxo, P., Müller, T., Wiedensohler, A., Paixão, M., Cirino, G. G., Arana, A., Swietlicki, E., Roldin, P., Fors, E. O., Wiedemann, K. T., Leal, L. S. M., and Kulmala, M.: Long term measurements of aerosol optical properties at a primary forest site in Amazonia, *Atmos. Chem. Phys.*, 13, 2391–2413, doi:10.5194/acp-13-2391-2013, 2013.
- Rummel, U., Ammann, C., Kirkman, G. A., Moura, M. A. L., Foken, T., Andreae, M. O., and Meixner, F. X.: Seasonal variation of ozone deposition to a tropical rain forest in southwest Amazonia, *Atmos. Chem. Phys.*, 7, 5415–5435, doi:10.5194/acp-7-5415-2007, 2007.
- Seinfeld, J. H. and Pandis, S. N.: *Atmospheric Chemistry and Physics: from Air Pollution to Climate Change*, J. Wiley, New York, 1998.
- Sierra, C. A., Harmon, M. E., Moreno, F. H., Orrego, S. A., and Del Valle, J. I.: Spatial and temporal variability of net ecosystem production in a tropical forest: testing the hypothesis of a significant carbon sink, *Glob. Change Biol.*, 13, 838–853, 2007.
- Sigler, J. M., Fuentes, J. D., Heitz, R. C., Garstang, M., and Fisch, G.: Ozone dynamics and deposition processes at a deforested site in the Amazon Basin, *Ambio*, 31, 21–27, 2002.
- Sitch, S., Cox, P. M., Collins, W. J., and Huntingford, C.: Indirect radiative forcing of climate change through ozone effects on the land-carbon sink, *Nature*, 448, 791–795, 2007.
- Taylor, J. A. and Lloyd, J.: Sources and sinks of atmospheric CO<sub>2</sub>, *Aust. J. Bot.*, 40, 407–418, 1992.
- Taylor, K. E., Stouffer, R. J., and Meehl, G. A.: An overview of CMIP5 and the experiment design, *B. Am. Meteorol. Soc.*, 93, 485–498, 2012.
- The HadGEM2 Development Team: G. M. Martin, Bellouin, N., Collins, W. J., Culverwell, I. D., Halloran, P. R., Hardiman, S. C., Hinton, T. J., Jones, C. D., McDonald, R. E., McLaren, A. J., O'Connor, F. M., Roberts, M. J., Rodriguez, J. M., Woodward, S., Best, M. J., Brooks, M. E., Brown, A. R., Butchart, N., Dearden, C., Derbyshire, S. H., Dharssi, I., Doutriaux-Boucher, M., Edwards, J. M., Falloon, P. D., Gedney, N., Gray, L. J., Hewitt, H. T., Hobson, M., Huddleston, M. R., Hughes, J., Ineson, S., Ingram, W. J., James, P. M., Johns, T. C., Johnson, C. E., Jones, A., Jones, C. P., Joshi, M. M., Keen, A. B., Liddicoat, S., Lock, A. P., Maidens, A. V., Manners, J. C., Milton, S. F., Rae, J. G. L., Ridley, J. K., Sellar, A., Senior, C. A., Totterdell, I. J., Verhoef, A., Vidale, P. L., and Wiltshire, A.: The HadGEM2

19976

- family of Met Office Unified Model climate configurations, *Geosci. Model Dev.*, 4, 723–757, doi:10.5194/gmd-4-723-2011, 2011.
- Thompson, T. M. and Selin, N. E.: Influence of air quality model resolution on uncertainty associated with health impacts, *Atmos. Chem. Phys.*, 12, 9753–9762, doi:10.5194/acp-12-9753-2012, 2012.
- 5 Tie, X., Brasseur, G., and Ying, Z.: Impact of model resolution on chemical ozone formation in Mexico City: application of the WRF-Chem model, *Atmos. Chem. Phys.*, 10, 8983–8995, doi:10.5194/acp-10-8983-2010, 2010.
- Valari, M. and Menut, L.: Does an increase in air quality models' resolution bring surface ozone concentrations closer to reality?, *J. Atmos. Ocean. Tech.*, 25, 1955–1968, 2008.
- 10 van der Werf, G. R., Randerson, J. T., Giglio, L., Collatz, G. J., Mu, M., Kasibhatla, P. S., Morton, D. C., DeFries, R. S., Jin, Y., and van Leeuwen, T. T.: Global fire emissions and the contribution of deforestation, savanna, forest, agricultural, and peat fires (1997–2009), *Atmos. Chem. Phys.*, 10, 11707–11735, doi:10.5194/acp-10-11707-2010, 2010.
- 15 Wesely, M. L.: Parameterization of surface resistances to gaseous dry deposition in regional-scale numerical models, *Atmos. Environ.*, 23, 1293–1304, 1989.
- Yienger, J. J. and Levy II, H.: Global inventory of soil-biogenic  $\text{NO}_x$  emissions, *J. Geophys. Res.*, 100, 11447–11464, 1995.

19977

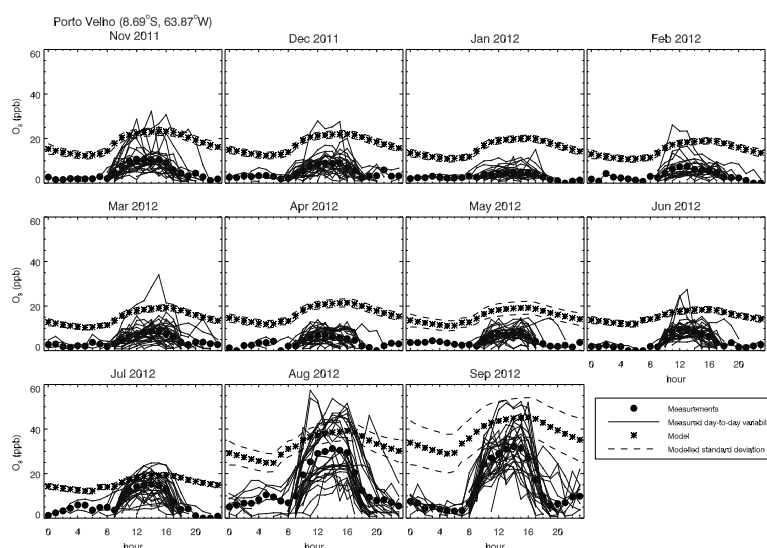


**Figure 1.** Comparison of measured and simulated monthly averaged diurnal cycle of surface  $\text{O}_3$  mixing ratios at the Porto Velho site, including measured day-to-day variability and standard deviation for the model results. The measurements have an uncertainty of 4%.

19978

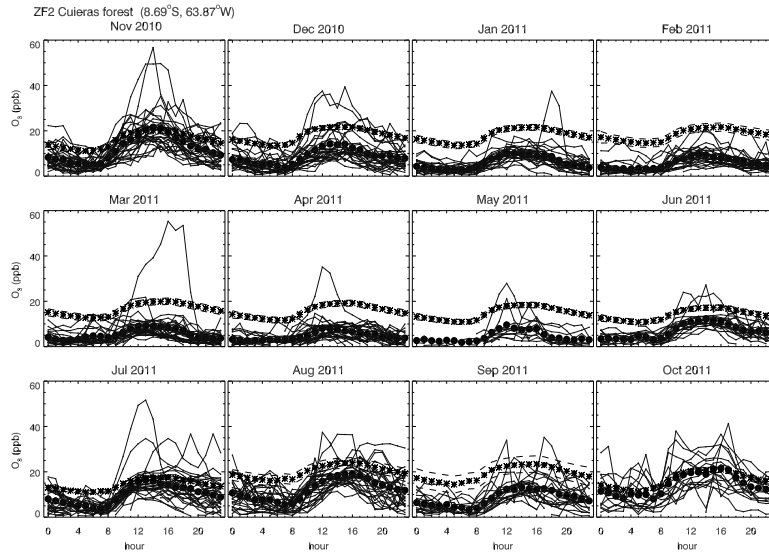


**Figure 2.** Comparison of measured and simulated monthly averaged diurnal cycle of surface  $O_3$  mixing ratios at the ZF2 site in the Cuieras forest reserve, including measured day-to-day variability and standard deviation for the model results. The measurements have an uncertainty of 4%. We show one of the two available years of observations. Legend as in Fig. 1.

19979

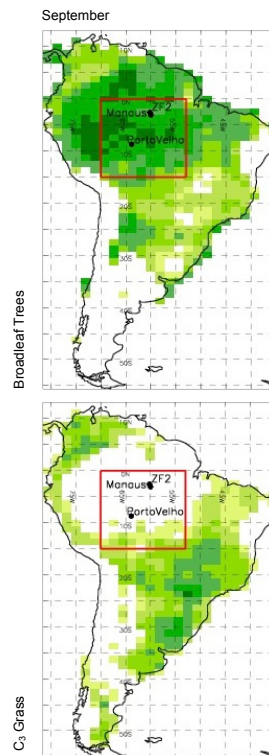


**Figure 3.** Vegetation cover in HadGEM2 for the month of September. The red rectangle is our region of analysis. The two sites used in the model evaluation (the sites of Porto Velho and ZF2 site in the Cuieras forest reserve) are also marked.

19980

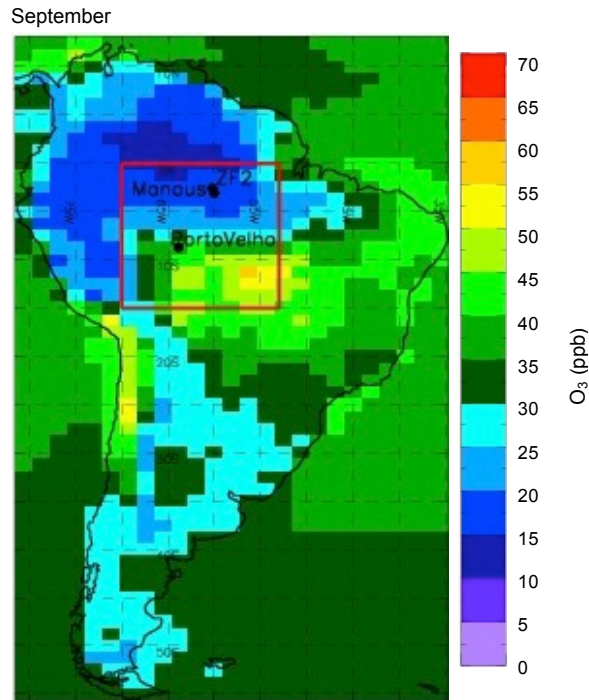


**Figure 4.** Monthly average surface O<sub>3</sub> mixing ratio simulated with HadGEM2 for the month of September (average over 8 years of simulations).

19981

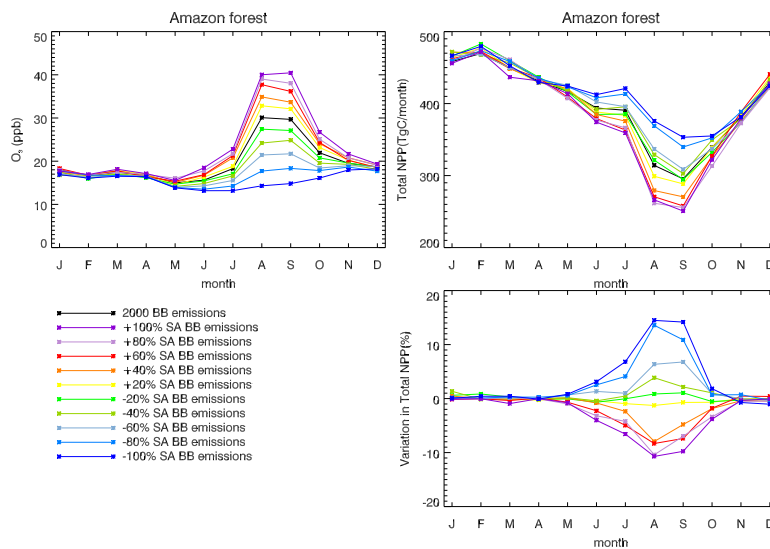


**Figure 5.** Clockwise from the top-left: **(a)** simulated monthly surface O<sub>3</sub> mixing ratios; **(b)** simulated monthly total NPP; **(c)** simulated monthly variation in total NPP. The plots show the results for the control simulation (i.e. using the decadal mean biomass burning emissions from Lamarque et al. (2010) centered on year 2000; 2000 BB emissions) and the various experiments with increased (+) or decreased (-) biomass burning emissions over South America (SA BB emissions) by 20, 40, 60, 80 and 100%. All data are averaged over the region of analysis for 8 years of simulations.

19982

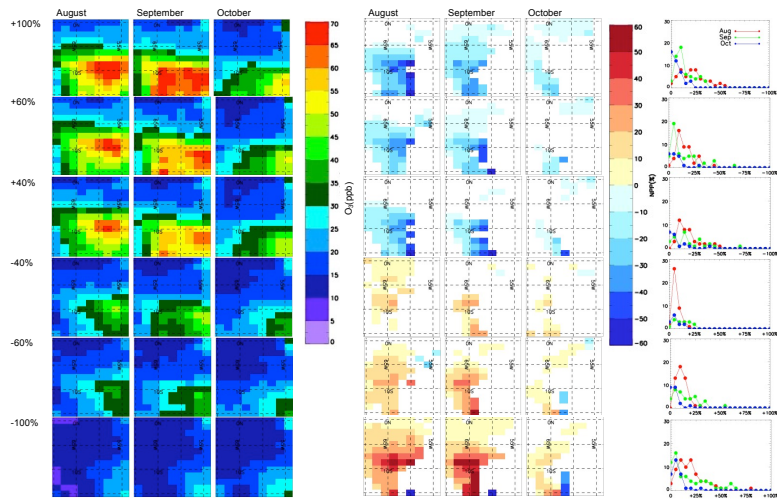


**Figure 6.** From the left: simulated variation in surface O<sub>3</sub> mixing ratios **(a)** and NPP **(b)** over the region of analysis for the months of August, September and October. **(c)** Probability density function (histogram) of the variation in NPP for the same months. The plots show the variation between the experiments with South American biomass burning increased/decreased by 40, 60 and 100 % and the control simulation.